2009 Ninth International Conference on Intelligent Systems Design and Applications

Cluster Analytic Detection of Disgust-Arousal

Masood Mehmood Khan
Faculty of Science and Engineering, Curtin University of Technology
Perth, Western Australia
Masood.Khan@curtin.edu.au

Abstract

Automated detection of disgust-arousal could have applications in diagnosing and treating obsessive-compulsive disorder and Huntington's disease. For achieving this ability, experimental data was used first to examine the thermal response of "facial muscles of disgust" to other common negative and positive expressions of emotive states. An attempt was then made to detect disgust-arousal through classification of affect-educed thermal variations measured along the facial muscles. Initial results suggest (i) muscles of disgust experience different levels of thermal variations under the influence of various emotive state and (ii) emotion-educed facial thermal patterns can be modeled as stochastically independent clusters to be separated as linear spaces and making automated detection of disgust-arousal possible.

1. Introduction

Automated detection of disgust-arousal has potential applications in the realms of psychology and psychiatry [1,2]. For example, automated detection of disgust-arousal is believed to be useful in therapeutic treatment of obsessive-compulsion disorder (OCD) and Huntington's disease [1,2]. Several recent investigations have therefore focused on computer-assisted detection of disgust-arousal and physiology-based measurement of disgust-sensitivity [1].

Disgust, an aversive emotive state, is considered a basic emotion [1]. The raised upper lips, wrinkled nose and raised lower eye-lids typically engage a set of facial muscles: *corrugator, orbicularis oculi* and *levator labii superioris* to (visually) characterize the expression of disgust [3,4]. The so called facial muscles of disgust are shown in Figure 1. Somatically, disgust is associated with nausea, heart rate decrease and low blood pressure [1]. Though disgust-arousal results in a distinct pattern of Psychophysiological response [1,2] its automated detection and recognition have so far been complex and tedious [5,6].

Previous works on disgust-arousal detection have utilized phenomena such as skin conductance, blood volume flow, pulse and electrical activity in brain [4]. These formats of human information are effective but bring with them several limitations. Firstly, they are often invasive. Secondly, it is often very difficult, on the basis of psychophysiological evidence alone, to make unambiguous interpretations of the meanings of detected changes. Furthermore, though the physiological signals can indicate the strength of a reaction to an event but identifying qualitative aspects, such as positive or negative emotional valence, is problematic. Both positive and negative emotions can cause similar changes in the levels of arousal, and researchers cite many instances of contradictory findings, such as observations of both increases and decreases in pulse rate as a result of increasing mental workload [7,8]. Finally, these techniques are considered expensive, laborious and time consuming [7].

Following the earlier work by Albert F. Ax [9], many researchers have reported influence of emotive states on the facial thermal features [10]. Studies have demonstrated that pixel grey-levels in thermal infrared images might provide a reliable measure of skin surface radiance and allow measuring the skin temperature distribution patterns [12,13]. Investigators were able to recognize the stress levels, deceit and facial expressions of positive and negative emotive states using the pixel grey-levels extracted from thermal images, though more frequently in a dichotomous discrimination manner [11,14-15]. Attempts were also made to classify the facial skin temperature measurements for non-invasive recognition of expressions of emotive states [11,14-15].

Some 140 years ago Darwin discovered that emotions have a universal facial expression [16]. Over a century later, Ekman and Friesen [3] investigated how the facial expression of emotion would engage the facial muscles. The facial muscles that typically engage in the expression of each emotive state

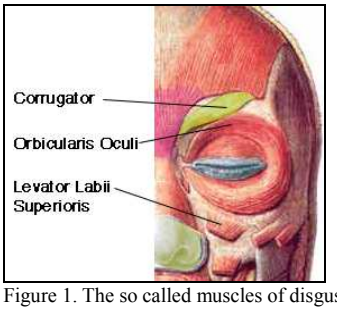

Figure 1. The so called muscles of disgust on a human face.

978-0-7695-3872-3/09 $26.00 © 2009 IEEE
DOI 10.1109/ISDA.2009.91

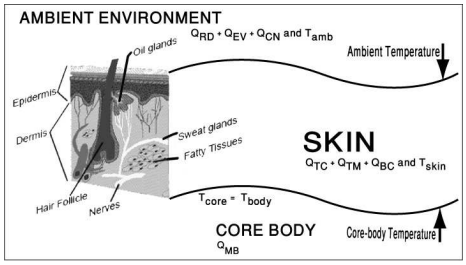

Figure 2. The human core-body to ambient environment heat transfer model.

belonging to the group of six basic emotions were thus identified [3]. However, little is known about the physiological changes that take place on these muscles under the influence of each of the common emotive state. Though several investigators have studied electrical variations that take place on the facial muscles under the influence of basic emotions using electromyography (EMG) [17-19], the hæmodynamic and thermal characteristics of facial muscles under the influence of common emotive states have yet to be investigated and understood.

This work, for the first time, examines how the muscles known to represent the expression of disgust: *corrugator, orbicularis oculi*, and *levator labii superioris* would respond to the other common negative (such as anger and sadness) and positive (such as happy) emotive states. The investigations focus on establishing if the non-invasive psychophysiological information processing would assist in distinguishing disgust from the expressions of other negative and positive emotive states. The scientific foundations of this work are summarized in the following section. The experiment design, employed feature extraction and selection method and initial results are then sequentially presented to analyze and discuss the results of this investigation.

2. Emotion-Educed Facial Skin Temperature Variations

The human skin temperature can be determined by measuring the amount of heat dissipated from the core body as a result of the blood volume flow, metabolic function, subcutaneous tissue structure and the sympathetic nervous activities [12,20]. Pennes's one-dimensional bio-heat transfer model [21] is usually employed to predict and estimate the amount of heat dissipated from the core body to the skin surface. Equation 1 represents the Pennes's model is as:

$$\rho c \frac{dT}{dt} = k\nabla^2 T + \rho_b c_b \omega_b (T_a - T) + q_{met} + q_{ext} . \quad (1)$$

The letters ρ, c and k represent the density, the specific heat and the thermal conductivity of blood respectively. T and T_a respectively denote the tissue and arterial blood temperatures, ω_b denotes tissue blood perfusion rate and, q_{met} and q_{ext} respectively represent the metabolic and external heat generation.

Assuming that the tissue properties are independent of tissue temperature and the human tissues are isotropic and homogenous, Pennes's bio-heat transfer equation can be simplified and adapted to develop a core-body to skin surface heat transfer model for estimating the emotion-specific temperature variations on the facial skin. Figure 2 exhibits a typical body heat and temperature flow model and explicates the flow of heat from the core body through the human skin. The heat generated inside the human body (Q_{BM}) is supposed to set the core body temperature (T_{body}). In a typical human body heat and temperature flow model, the body temperature (T_{body}) and the core body temperature (T_{core}) are assumed to be equal [12,20-22]. Three body heat-flux factors and three heat production factors determine the skin temperature. The three body heat-flux factors are: convection heat-flux (Q_{CN}), radiation heat-flux (Q_{RD}), and evaporation heat-flux (Q_{EV}). The body heat production depends on the heat conduction from the core body (Q_{TC}), body metabolism (Q_{TM}) and the amount of heat convection due to blood flow (Q_{BC}). Equation 2 exhibits how the thermal equilibrium is achieved on the skin surface under the neutral conditions [12,20-22].

$$(Q_{CN}) + (Q_{RD}) + (Q_{EV}) = (Q_{TC}) + (Q_{TM}) + (Q_{BC}) \quad (2)$$

When thermal imaging is employed to detect emotion-specific skin temperature variations, the time-sequential thermal images are analysed to determine the regional skin temperature variations and their associated transient changes in physiological functions [20]. Equation 2 allows comparing the amount of heat produced with the amount of dissipated heat in the time-sequential images. An imbalance between the two sides of Equation 2 suggests either heat loss or heat gain in the skin regions under investigation [20].

Studies suggest that a change in emotive state may cause some variation in the blood volume flow under the facial skin. It is argued that the facial expression of emotion results in musculo-thermal activities on the face. The emotion-educed blood volume flow variations and the musculo-thermal changes are believed to cause variations in the facial skin temperature [12,13]. Since, the facial expressions change rapidly, the effect of ambient temperature on the facial skin temperature may be ignored. Hence any imbalance observed between the two sides of Equation 2 may be attributed to the facial skin temperature gain or loss due to a change in the facial expression of emotion.

Assuming C_{skin} is the heat capacity of the facial skin, the facial skin temperature change (ΔT_{skin}) observed over a short time period (Δt) is expressed as:

$$C_{skin}\Delta T_{skin} = (Q_{TC}) + (Q_{TM}) + (Q_{BC}) - [(Q_{CN}) + (Q_{RD})\ (Q_{EV})] \quad (3)$$

Equation 3 allows calculating the skin temperature changes over a short time period due to a change in the expression of emotive states. Two thermograms, each recorded with a different facial expression may therefore be subtracted to determine the facial skin temperature changes within the regions of interest in the thermograms [12,20]. This image temperature subtraction method was employed in this work to compare facial thermal variations in thermograms with different facial expressions of affective states.

3. Experiment Design

For developing a set of 80 visible-spectrum and thermal images, a high-resolution video camera and an uncooled-microbolometer FPA detector mounted 320 × 240 pixels thermal infrared camera were used. The infrared camera had a high thermal sensitivity, 0.08 ºC at 30 ºC, with an accuracy of ± 2 ºC in the wavelength range of 7.50-14.00 µm. The internal room temperature was maintained between 19-22 ºC during the image acquisition. Each participant was given at least 20 minutes to acclimatize with the environment. A low emissivity (ε = 0.54) concrete wall background was used to ensure better separation of the background from the desired regions of the thermal images [13,22]. Participants included male and female Arab, Iranian and Indian students.

Emotions of happiness, sadness, disgust and anger were evoked using a set of selected still images and video clips. Extremely violent and disturbing images and images with unethical contents were avoided. The employed images and video clips had both high and low emotion evoking contents.

4. Feature Extraction and Selection

An attempt was made to remove any undesired noise from within the thermal infrared images (TIRIs). Many convolution methods are available to minimize the influence of noise factors [23]. The "median smoothing filter" recognized as a good best order-statistic filter, was invoked on the thermal images for noise reduction. The filter applies a non-liner solution approach for recovering the original image signals and results in excellent noise reduction with a minimal blurring [23]. Instead of averaging the pixels, the filter replaces value of a pixel by the median of the grey levels in the neighborhood of the pixel. The median value is therefore taken from one of the pixels within the neighborhood using the relationship,

$$\hat{f}(p,q) = \underset{(u,v)\in U_{pq}}{median}\,. \qquad (4)$$

In equation 4, $\hat{f}(p,q)$ is the median filter that replaces the value of a pixel (u, v) by the median of the grey levels within a defined neighborhood.

In a following image enhancement step, the Sobel operator-based edge detection algorithm was invoked for extracting the contours within the infrared images. For the selected 3x3 neighborhood, the gradient operators were calculated according as [23]:

$$Gu = [f(i-1,j-1) + 2f(i-1,j)] + f(i-1,j+1)] - [f(i+1,j-1) + 2f(i+1,j) + f(i+1,j+1)] \qquad (5)$$

and

$$Gv = [f(i-1,j-1) + 2f(i,j-1)] + f(i+1,j-1)] - [f(i-1,j+1) + 2f(i,j+1) + f(i+1,j+1)] \qquad (6)$$

The gradient magnitude could then be easily computed according as

$$G[f(u,v)] = \sqrt{Gu^2 + Gv^2}\,. \qquad (7)$$

4.1 Discovery of Thermally Significant Facial Points

The time-sequential TIRIs were analyzed through comparing the temperature measurements at the points of registration within a series of images to discover the transient and temporal changes in the temperature distributions. The temperature measurements taken at different sets of registration points within the TIRIs were analyzed to discover any temporal changes in the temperature distributions. The thermal intensity values (TIVs) were repeatedly measured at different sets of points to ensure a "minimum correlation among the data" and a "maximum between-facial expression" variance. The algorithmic process elaborated in [6,14-15,24] and shown in Figure 3 resulted in the discovery of significant thermal variations at 75 physical sites located all over the face along the major facial muscles within the TIRIs.

1	Symmetrically divide thermal image into N squares
2	Set $Correlations_{ST}$ = 0
3	Set $Variance_{ST}$ = 0
4	Set the list of FTFPs = Empty
5	***For*** squares 1 to N,
6	Find the highest level of grey in the square
7	Measure the corresponding temperature of the discovered highest grey level
8	Add the discovered highest temperature point to the list of FTFPs
9	Calculate the correlation between the FTFPs
10	Set the FTFP Correlation = Cor_{new}
11	Calculate the Variance between the FTFPs
12	Set the FTFP Variance = Var_{new}
13	**If** {(Cor_{new} > $Correlations_{ST}$) and (Var_{new} > $Variance_{ST}$)}
14	Then (($Correlations_{ST}$ = Cor_{new})And (Var_{new} = $Variance_{ST}$))
15	And Keep the newly discovered FTFP in the list of FTFPs
16	Else, Remove the newly discovered FTFP in the list of FTFPs
17	**End If**
18	***End For***

Figure 3. Significant Facial Thermal Feature Point Selection Procedure

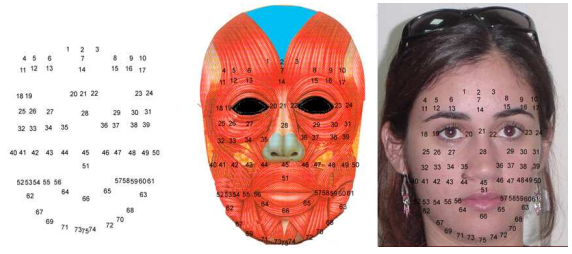

Figure 4. Left to right: Geometric profile of FTFPs, FTFPs on a facial muscle map and FTFPs on a human face

Figure 4 shows these 75 facial thermal feature points (FTFPs) on a human face, a muscular map of a human face, and the geometric profile of the facial thermal feature points. More than 50 % of these FTFPs were located on the five major facial muscles: Frontalis (16 FTFPs), Orbicularis Oculi Pars Orbital (12 FTFPs), Levator Labii Superioris (6 FTFPs) and Risorious (6 FTFPs) seem to hold 53.33% of the FTFPs on a human face. Table I shows the physical location of the FTFPs on the face. The TIV data recorded at the 75 FTFP sites were used to represent each thermal image as a 75-dimensional thermal feature vector for the subsequent investigation and analyses.

In a follow up analysis, the most effective of these FTFPs were discovered using Principal Component Analysis (PCA) a computationally inexpensive and robust feature extraction method [25].

5. Thermal Response of Muscles of Disgust to Common Emotive States

Figure 5 suggests that the two so called muscles of disgust: *lavatory labii superioris and orbicularis oculi* experience much higher thermal variation when disgust is being expressed than they would when any other emotive state is expressed. However, our experimental data shows that one 'important' muscle of disgust, *corrugator*, would experience much higher thermal variation under the influence of anger as compare to the expression of disgust. Nonetheless, the thermal variations observed on *corrugator* under the influence of disgust were much higher then those observed under the influence of sadness and happiness.

TABLE I. PHYSICAL LOCATION OF FTFPS ON THE FACE

Part of the face	FTFPs
Forehead	1, 2, 3, 4, 5, 6, 7, 8, 9, 10
Around the eyes	11, 12, 13, 14, 15, 16, 17, 18, 19, 20, 21, 22, 23, 24, 25, 26, 27, 28, 29, 30, 31
Cheeks	32, 33, 34, 35, 36, 37, 38, 39, 40, 41, 42, 43, 47, 48, 49, 50, 62, 63
Around mouth	44, 45, 46, 51, 52, 53, 54, 55, 56, 57, 58, 59, 60, 61, 64, 65, 66

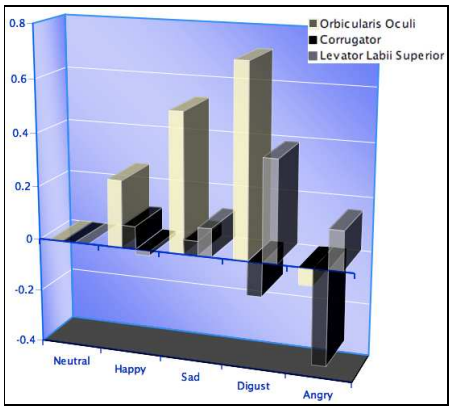

Figure 5. Thermal variations observed on the "muscles of disgust" under the influence of negative and positive expressions of emotive states

6. Initial Analysis of Facial Thermal Data

The thermal data were transformed into a set of uncorrelated principal components using the transformation techniques suggested in [25].

Figure 6 exhibits the discovered possible separation between the neutral and invoked facial expressions of happiness in a 2-principal component eigenspace.

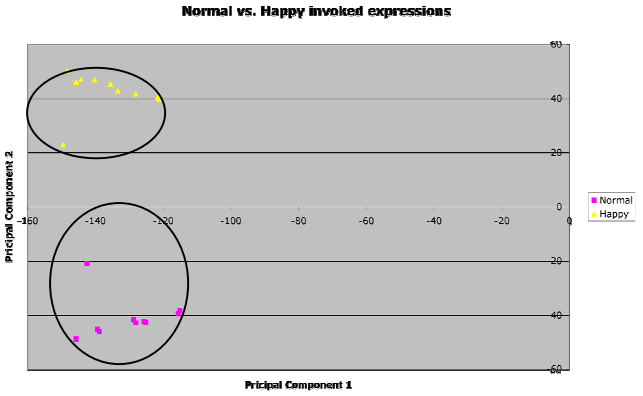

Figure 6.Separation of the neutral faces and evoked expression of happiness in a 2-PC eigenspace

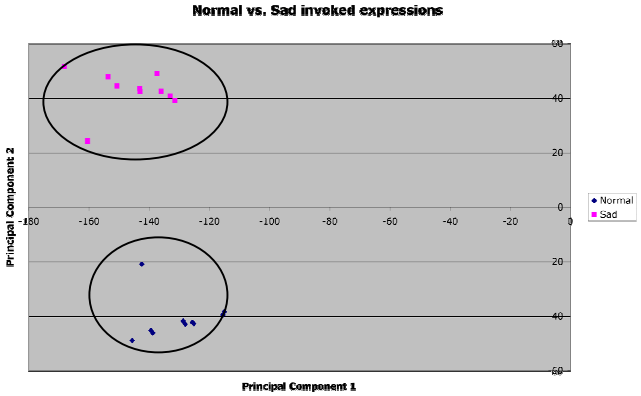

Figure 7. Separation of neutral faces and evoked expression of sadness in a 2-PC eigenspace

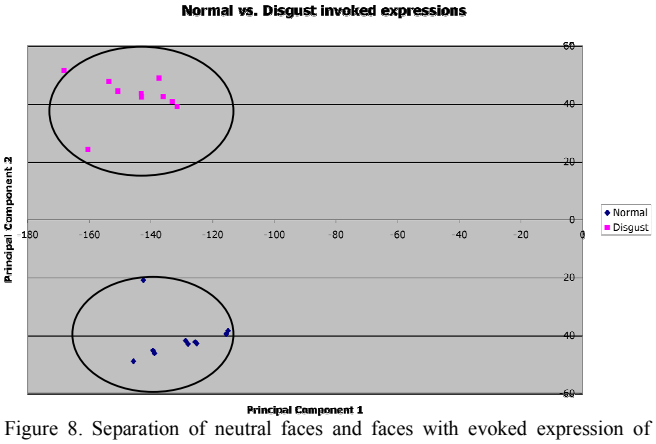

Figure 8. Separation of neutral faces and faces with evoked expression of disgust in a 2-PC eigenspace

Figure 7 exhibits how the neutral and the sad faces were separated in a 2-component eigenspace.

Figure 8 shows how the neutral faces and the faces with the evoked expression of disgust were separated in a 2-principal component eigenspace.

Figure 9 exhibits the separation between the neutral faces and faces with the evoked facial expression of anger in the 2-principal component eigenspace. Figures 6 to 9 provide some convincing information about the differences in the thermal profiles of the neutral faces and the faces with evoked facial expressions. It is obvious in the four figures that a face expressing disgust-arousal has a unique and different thermal pattern than a neutral face or a face that expresses any other positive or negative effective state.

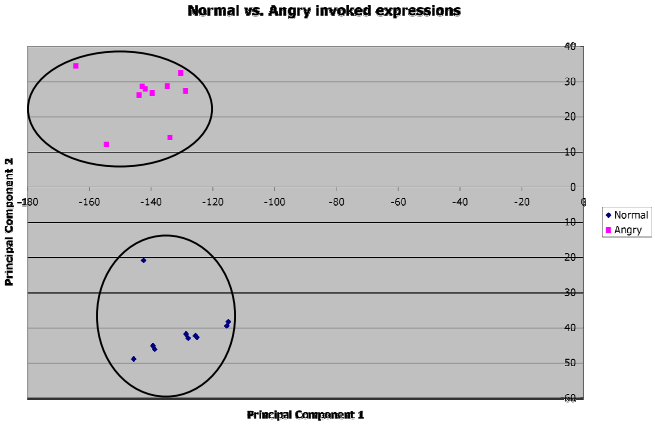

Figure 9. Separation of the neutral faces and evoked expression of anger in a 2-PC eigenspace

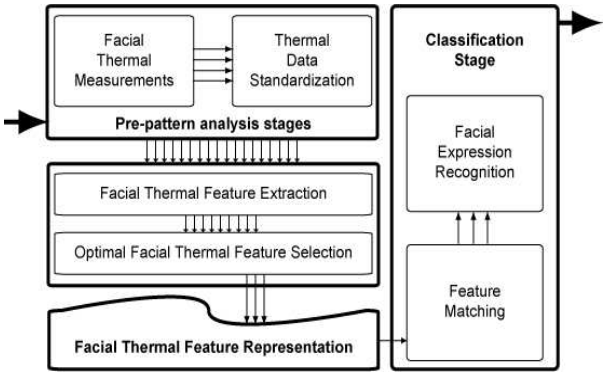

Figure 10. The employed pattern analysis schema

TABLE II. **SUCCESS MATRIX FOR THE CROSS-VALIDATION OF FACIAL EXPRESSION CLASSIFICATION RESULTS

Facial Exp. Group	Predicted Group Membership					Total
	Neutral	*Happy*	*Sad*	*Disgust*	*Angry*	
Neutral	70.0	0	0	(10.0)	(20.0)	**100**
Happy	0	70.0	(20.0)	(10.0)	0	**100**
Sad	0	(10.0)	90.0	0	0	**100**
Disgust	(10.0)	(10.0)	0	70.0	(10.0)	**100**
Anger	(20.0)	0	0	(20.0)	60.0	**100**

** Confusion patterns are reported in parenthesis

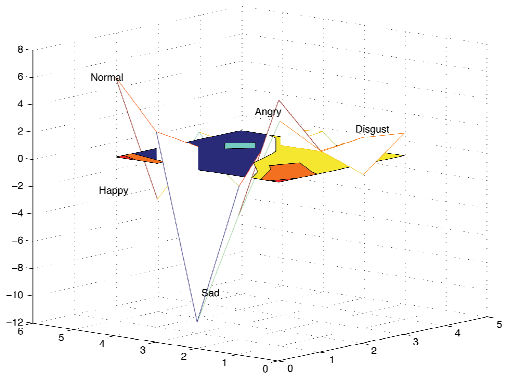

Figure 11. The neutral faces and the faces with four evoked facial expressions at their respective group centroids

7. Classifier Design

A pattern analysis schema, reported earlier in [17,14,15,24] and exhibited in Figure 10, was employed for classifying the facial thermal feature patterns.

The uncorrelated principle components were examined for their contribution in the overall variance in the thermal data. The ratio of within and between group variance ($|S_B|/|S_W|$)was used as a criterion for keeping the most discriminating facial thermal components termed "optimal features" in the classifier training feature set.

For pattern classification, linear discriminant analysis (LDA) was invoked on the optimal features. LDA has been successfully used in several related investigations. It works at three levels for optimally dividing a Gaussian like feature space into linear regions of interest. At the first level, it identifies the variables that best separate each cluster in a training sample from the rest of the sample. On the second level, LDA uses the identified variables to define and compute new functions of input data. It does so by parsimoniously projecting the between-cluster differences. At the third level, LDA uses the discriminant functions to classify any future observations [26]. In essence, LDA seeks a linear space to maximize the between-group separation. Since there were K optimal features in the optimal learning set, the between-cluster separation measure J_K would allow quantifying the discrimination power of the training features [26-28].

8. Results

Figure 11 exhibits how the neutral faces, the faces expressing disgust, and the faces with expressing the two other (two negative and a positive) facial expressions set as clusters in an optimized eigenspace.

Interestingly, the negative facial expressions of anger and disgust were closer even in a compact thermal eigenspace. This observed "pattern of proximity" of these two (negative) emotive states has been reported in several studies that used either visual observations or brain signals for separating the

clusters of various emotive states in an eigenspace to detect disgust-arousal.

Table II, earlier reported as part of a larger study in [15], exhibits the classification success rates and the confusion patterns observed when the optimal features were employed to train the classifier and distinguish between the facial expressions of positive and negative emotive states. Please note that Table II reports only the conservative leave-one out classification results. Given a small sample size, the overall classification success rate (72.0%) observed during the conservative leave-one-out cross validation tests seems highly encouraging. The observed confusion patterns evident in parenthesis in Table II were also similar to those observed earlier in studies that employed facial physiognomy for automated facial expression classifier.

9. Conclusion

This work demonstrates that the so called "facial muscles of disgust" undergo some significant thermal changes in order to express the common emotive states. Distinguishing the common expressions of affective states from a neutral face using facial thermal features seems to be a lot easier than distinguishing between the emotive states. However, the thermal data analyses and classification results suggest that the facial thermal features measured along the major facial muscles might help in automated detection of disgust-arousal. However, the thermal data collected from the known and so-called "facial muscles of disgust" alone would not help in automated realization and recognition of disgust-arousal [6,14,24].

The observed classification results were consistent with the previous studies carried out to investigate the relationship between the emotions and the facial musculo-physiological activities. However, more work is needed to investigate the influence of age, gender and ethnicity related differences on the employed automated disgust detection approach. Also, an extended database of thermal and visual images would be required to validate the observed classification results.

10. References

[1] D. Vaitl, A. Scienle, and R. Stark, "Neurobiology of fear and disgust," *Int. Journal of Psychophysiology,* vol. 57, pp. 1-4, 2005.

[2] J. Gary, *Neurophysiology of anxiety*. New York: Oxford University Press, 1985.

[3] P. Ekman and W.V. Friesen, *Facial Action Coding System: A technique for the measurement of facial movement,* Pal Alto: Consulting Psychology Press, 1978.

[4] K. Wolf, R. Mass, T. Ingenbleek, F. Kiefer, D. Naber, D. and K. Wiedemann, "The facial pattern of disgust, appetence, excited joy and relaxed joy: An improved facial EMG study", *Scandinavian Journal of Psychology*, vol. 46, pp.403-409, October2005.

[5] P. Wright, G. Shapira He, W.K., Goodman, and Y. Liu, "Disgust and the insula: fMRI responses to pictures of mutilation and contamination," *NeuroReport*, vol. 15, pp. 2347–2351, 2004.

[6] M.M. Khan, "Cluster-analytic classification of facial expressions using infrared measurements of facial thermal features," Ph.D. Thesis, School of Computing & Engineering, University of Huddersfield, UK, 2008.

[7] R.W. Picard, E. Vyzas, and J. Healey, "Toward machine emotional intelligence: Analysis of affective physiological state," *IEEE Transactions on Pattern Analysis, Machine Intelligence*, vol. 23, no. 10, pp. 1175-1191, 2001.

[8] R.D. Ward, and P.H. Marsden, "Affective computing: problems, reactions and intentions", *Interacting with Computers*, vol. 16, no. 4, pp. 707-713, 2004.

[9] A.F. Ax, "The physiological differentiation between fear and anger in humans," *Psychosomatic Medicine,* vol. 15, No. 5, pp. 433-442, 1953.

[10] J.T. Cacioppo, D.J. Klein, G.G. Bernston, and E. Hatfield, "The psychophysiology of emotion," in Handbook of Emotions, M. Lewis and J.M. Haviland, Eds., New York: Guildford Press, 1993, pp. 119-142.

[11] I. Pavlidis and J. Levine. "Thermal image analysis for polygraph testing," *IEEE Engineering in Medicine and Biology*, vol. 21, no.6, pp. 56-64, 2002.

[12] M. Bales, "High-resolution infrared technology for soft –tissue injury detection," *IEEE Engineering in Medicine and Biology*," vol. 17, 1998, pp. 56-59.

[13] K. Otsuka, S. Okada, M. Hassan, T. Togawa, "Imaging of skin thermal properties with estimation of ambient radiation," *IEEE Engineering in Medicine and Biology*, vol. 21, no. 6, pp. 49-55, 2002.

[14] M.M. Khan, M. Ingleby and R.D. Ward, "Automated facial expression classification and affect interpretation using infrared measurement of facial skin temperature variation," *ACM Transactions on Autonomous and Adaptive Systems,* vol. 1, no. 1, pp. 91-113, 2006.

[15] M.M. Khan, R.D. and Ward M. Ingleby, "Classifying pretended and evoked facial expression of positive and negative affective states using infrared measurement of facial skin temperature," *ACM Transactions on Applied Perception*, vol. 6, no. 1, pp. 6:1-22, 2009.

[16] C. Darwin, *The expression of emotion in man and animals*. London: Murray, 1872.

[17] P. Ekman, R.W. Levenson and W.V. Friesen, "Autonomic nervous system activity distinguishes among emotions," *Science*, vol. 221, pp. 1208-1210, 1983.

[18] U. Dimberg, "Facial electromyography and emotional reactions," *Psychophysiology*, vol. 27, no. 5, pp. 481-494, 1990.

[19] B. Wild, M. Erb and M. Bartels, "Are emotions contagious? Evoked emotions while viewing emotionally expressive faces: quality, quantity, time course and gender differences," *Psychiatry Research*, vol. 102, pp. 109-124, 2001.

[20] I. Fujimasa, "Pathophysiological expression and analysis of infrared thermal images," *IEEE Engineering in Medicine and Biology*, vol. 17, no. 4, pp. 34-42, 1998.

[21] H.H. Pennes, "Analysis of tissue and arterial blood temperature in resting human forearm", *Journal of Applied Physiology,* vol.1, pp. 93-102, 1948.

[22] B.F. Jones and P. Plassmann, "Digital infrared thermal imaging of human skin," *IEEE Engineering in medicine and biology*, vol. 21, no.6, pp. 41-48, 2002.

[23] R.C. Gonzalez and R.E. Woods, *Digital Image Processing*. New York: Addison-Wesley, 2002.

[24] M.M Khan, R.D. Ward, and M. Ingleby, "Infrared thermal sensing of positive and negative facial expressions," *in the proc of the IEEE 2006 Conference on Robotics, Automation and Mechatronics*, Bangkok, Thailand, June 2006, pp. 406-411.

[25] I.T. Jolliffe, *Principal Component Analysis*, New York: Springer-Verlag, 2002.

[26] B.S. Everitt and G. Dunn, *Applied Multivariate Data Analysis*, London: John Wiley and Sons, 1991.

[27] I.T. Jolliffe, *Principal Component Analysis,* New York: Springer-Verlag. 2002.

[28] J.G. McLachlan, *Discriminant Analysis and Statistical Pattern Recognition,* New Jersey: Wiley & Sons, 2004.

Filename: Disgust-paper-ISDA-V06-Final_submit-4.doc
Directory: D:\2009-Conference-papers-to-go\2009-ISDA-Italy\Disgut-detect
Template: D:\Documents and Settings\239808C\Application Data\Microsoft\Templates\Normal.dot
Title: Paper Title (use style: paper title)
Subject:
Author: IEEE
Keywords:
Comments:
Creation Date: 10/09/2009 11:32:00 AM
Change Number: 5
Last Saved On: 10/09/2009 11:33:00 AM
Last Saved By: Faculty of Engineering and Computing
Total Editing Time: 1 Minute
Last Printed On: 10/09/2009 12:00:00 PM
As of Last Complete Printing
Number of Pages: 6
Number of Words: 3,970 (approx.)
Number of Characters: 22,633 (approx.)